

SURFACE NANOSTRUCTURE AND CATALYSIS: THE ROLE OF CONFINEMENT AND SURFACE CHEMISTRY

- Keith E. Gubbins¹, Erik E. Santiso¹, Liping Huang^{1,2} and Marco Buongiorno Nardelli²

- Center for High Performance Simulation

- Departments of Chemical and Biomolecular Engineering¹ and Physics², North Carolina State University, Raleigh, NC 27695, U.S.A.

- OUTLINE

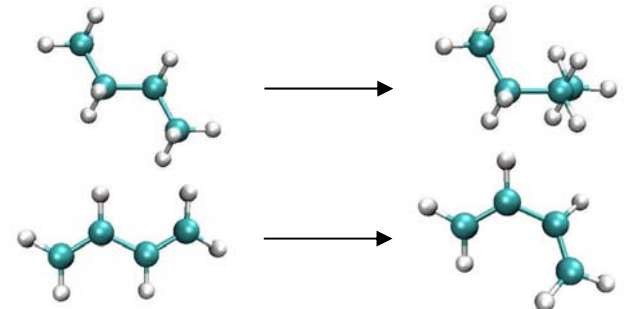
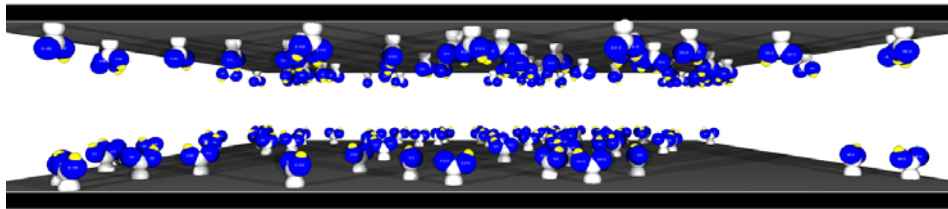
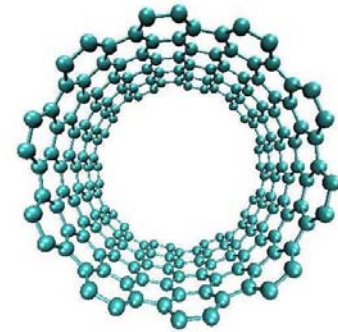
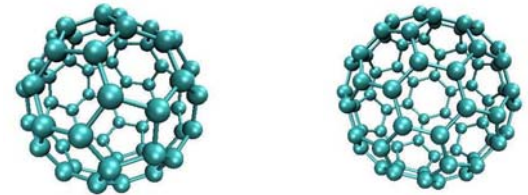
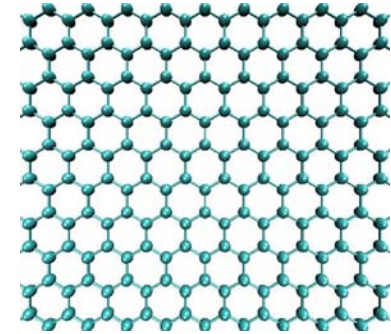
- Molecular level methods for studying reactions
- Effects of confinement on equilibrium composition
- Effects on reaction mechanism. Influence of (a) confinement geometry; (b) soft (dispersion) interactions; (c) strong interactions; (d) defects.
- Future needs

Nanostructure, Confinement and Chemical Reactions

- Chemical reactions are often carried out in micro- and nanoporous materials, in reverse micelles, nano-composites, on nanoparticles, in gels, and other nanostructured materials.
- Factors that can influence reactions in confinement include:
 - Strong interactions with the pore walls that affect the mechanism
 - Selective adsorption of reactants/products
 - Geometrical constraints
 - Electronic perturbation due to substrate
 - Large area/volume
 - Defects, surface curvature have a large effect on reactions
 - Increased density of the pore phase
- These factors can modify the equilibrium distribution of reactants and products, the reaction rate, and even the reaction mechanism.

Introduction

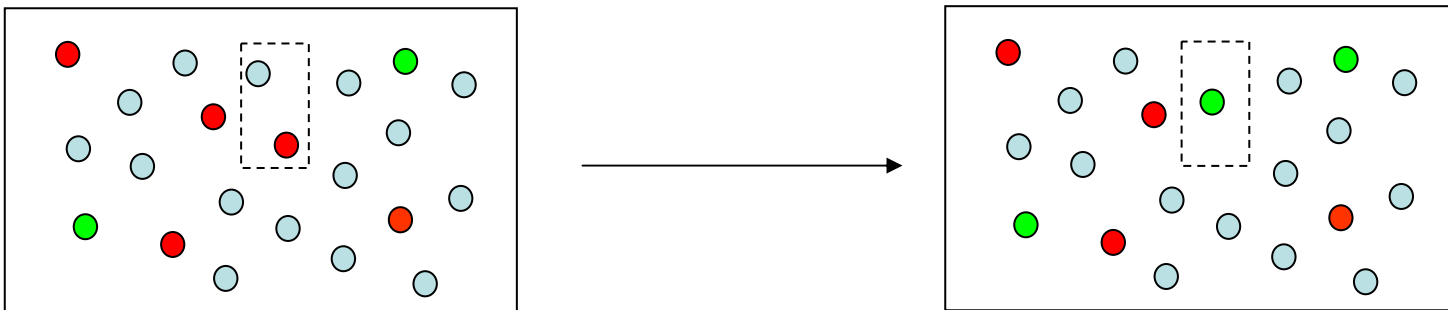
- Porous material - graphitic carbon:
 - Simple, abundant and easy to model
 - Flexible - can explore different geometries (graphene walls, nanotubes, nanohorns, other fullerenes)
 - Can modify reactivity in various ways: doping, addition of functional groups or transition metal atoms, structural defects, etc. – may be useful for designing a “super-catalyst” that takes advantage of shape-catalytic *and* chemical effects?



The 'Easy Part': Chemical Equilibrium

- Reactive Monte Carlo¹ (RxMC): In addition to the “standard” Monte Carlo moves, a set of “forward” and “backward” reaction moves are used. In these moves, reactant molecules are randomly chosen and replaced with product molecules (or vice versa).
- Acceptance probability for a “reactive” move is:

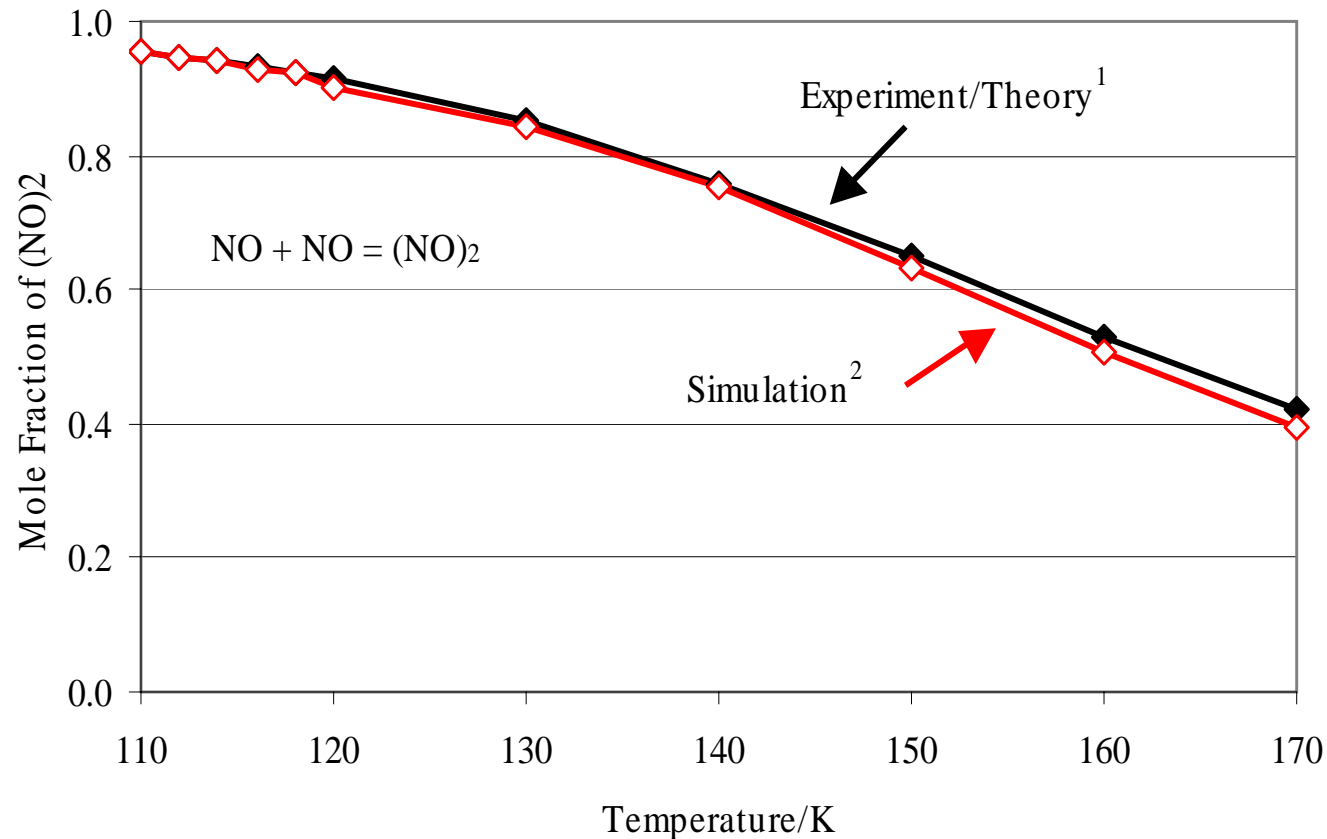
$$P_{acc} = \min \left\{ 1, \exp(-\beta\Delta\mathcal{U}) \prod_{i=1}^c q_i^{v_i} \frac{N_i!}{(N_i + v_i)!} \right\}$$



¹Johnson, J.K., Panagiotopoulos, A.Z., Gubbins, K.E., *Mol. Phys.* **81**, 717 (1994); J.K. Brennan, M. Lisal, K.E. Gubbins and B.M. Rice, *Physical Review E*, **70**, 061103 (2004).

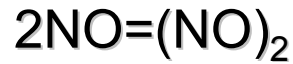
Dimerization of Nitric Oxide

- Bulk Saturated Liquid Phase



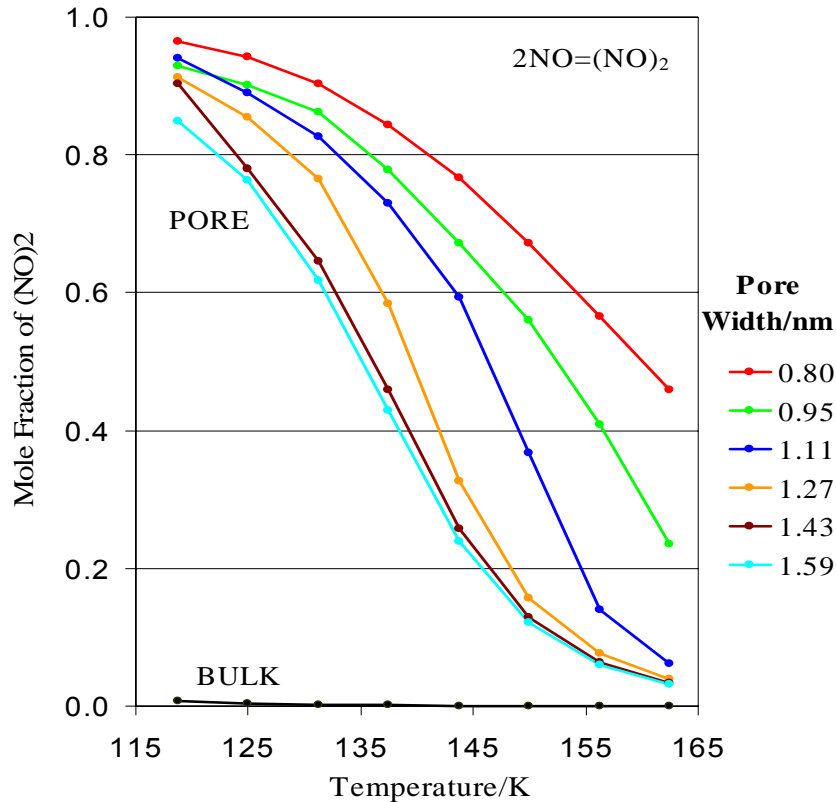
1. A. L. Smith and H. L. Johnston, *J. Am. Chem. Soc.*, 74, 1952.; H. J. R. Guedes, PhD thesis, Universidade Nova de Lisboa, Portugal, 1988.
2. C. H. Turner, J. K. Johnson, and K. E. Gubbins, *J. Chem. Phys.* 114(4), 2001.

Equilibrium: Dimerization of Nitric Oxide

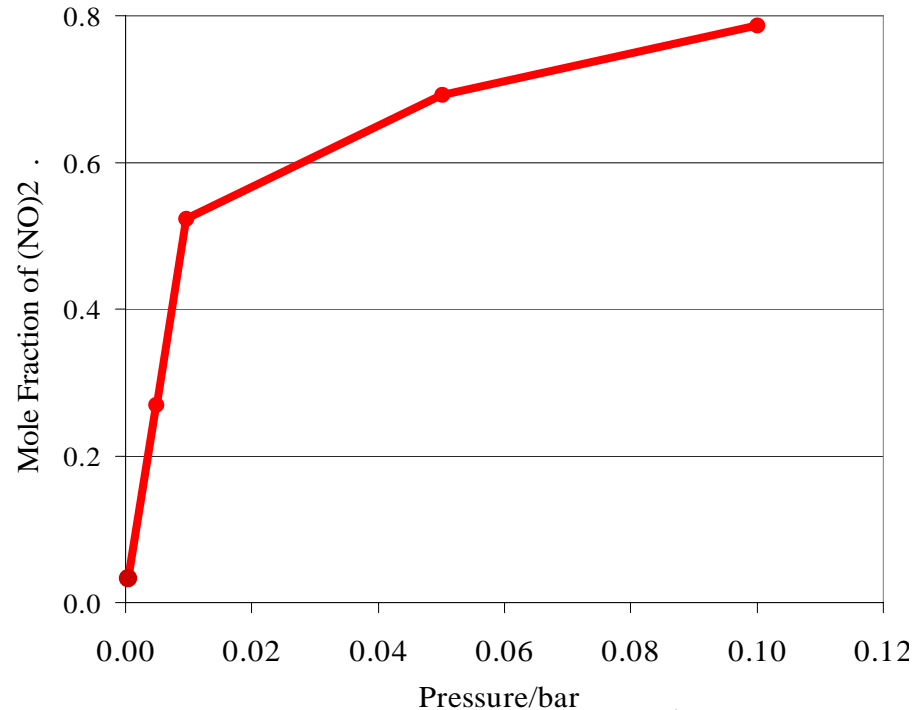


- Slit pores

- (10,10) Carbon nanotubes



$P=0.1$ bar



$T=130$ K

Theory: C. H. Turner, J. K. Johnson, and K. E. Gubbins, *J. Chem. Phys.* **114**, 1851 (2001).

Expt: O. Byl, P. Kondratyuk & J.T. Yates, Jr., *J. Phys. Chem. B* **107**, 4277 (2003); $x_{(\text{NO})_2} = 0.95 \pm 0.05$.

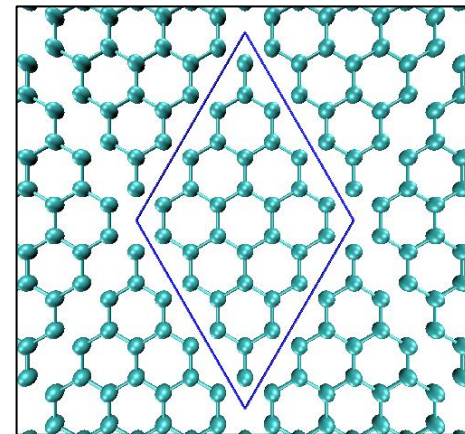
Modeling Chemical Reactions: Mechanism and Rates

Approach:

- Determine the Potential Energy Surface (PES) using electronic structure methods (e.g. density functional theory, DFT); use optimization methods to determine the important points on the reaction path (e.g. Nudged Elastic Band, Liao-Parinello). Phonon calculations enable us to determine the Free Energy Surface and hence temperature effects. Can also carry out Car-Parrinello Molecular Dynamics.
- Reaction rates, slow diffusion processes: These are rare events in the molecular scale (can be 10 or more orders of magnitude slower than molecular motions). For reactions with high activation energies can use Transition State Theory. Lower activation barriers require rare event techniques (e.g. “Blue Moon” MD, Bennett/Chandler MD).
- Multiple possible mechanisms - Require more advanced techniques to sample potential energy (or free energy) surface (e.g. Transition Path Sampling, Car-Parrinello MD)

Methods

- Density functional theory calculations:
 - Plane wave pseudopotential calculations using CPMD and pwscf¹.
 - Becke-Lee-Yang-Parr (BLYP) exchange-correlation.
 - Ultrasoft pseudopotentials.
- Partitioned rational function optimization (P-RFO) to obtain the structure of transition states.
- Carbon walls modeled as 32-atom graphene sheets on a hexagonal unit cell.
- ParFuMS code (beta) to estimate effect of temperature².
- Variational Transition State Theory (VTST) or BMMD to estimate rate constants.



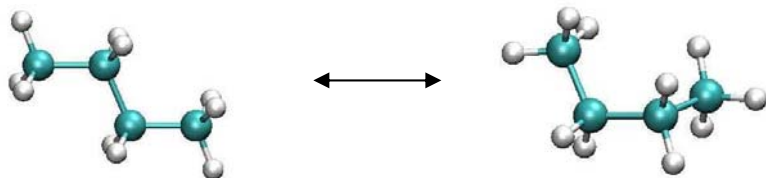
¹CPMD, © IBM Corp. 1990-2003, © MPI für Festkörperforschung Stuttgart 1997-2001, <http://www.cpmd.org>
PWSCF, S. Baroni, A. Dal Corso, S. de Gironcoli, and P. Giannozzi, <http://www.pwscf.org>

²Partition Functions of Molecules and Solids (ParFuMS) E.E. Santiso 2006-2007,
<http://gubbins.ncsu.edu/users/erik/parfums/>

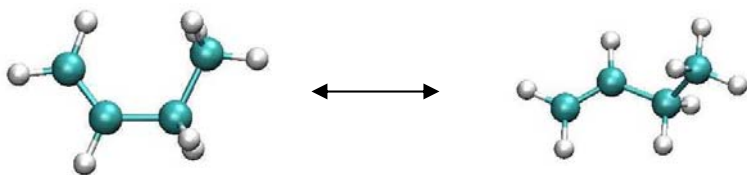
Geometric Constraints: C4 Hydrocarbons

- Three examples (gas phase):

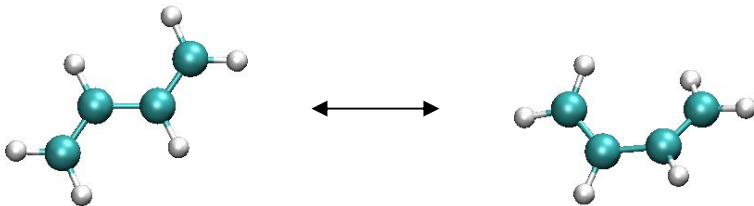
- Isomerization of n-butane - *anti* \leftrightarrow *gauche* (*syn*)



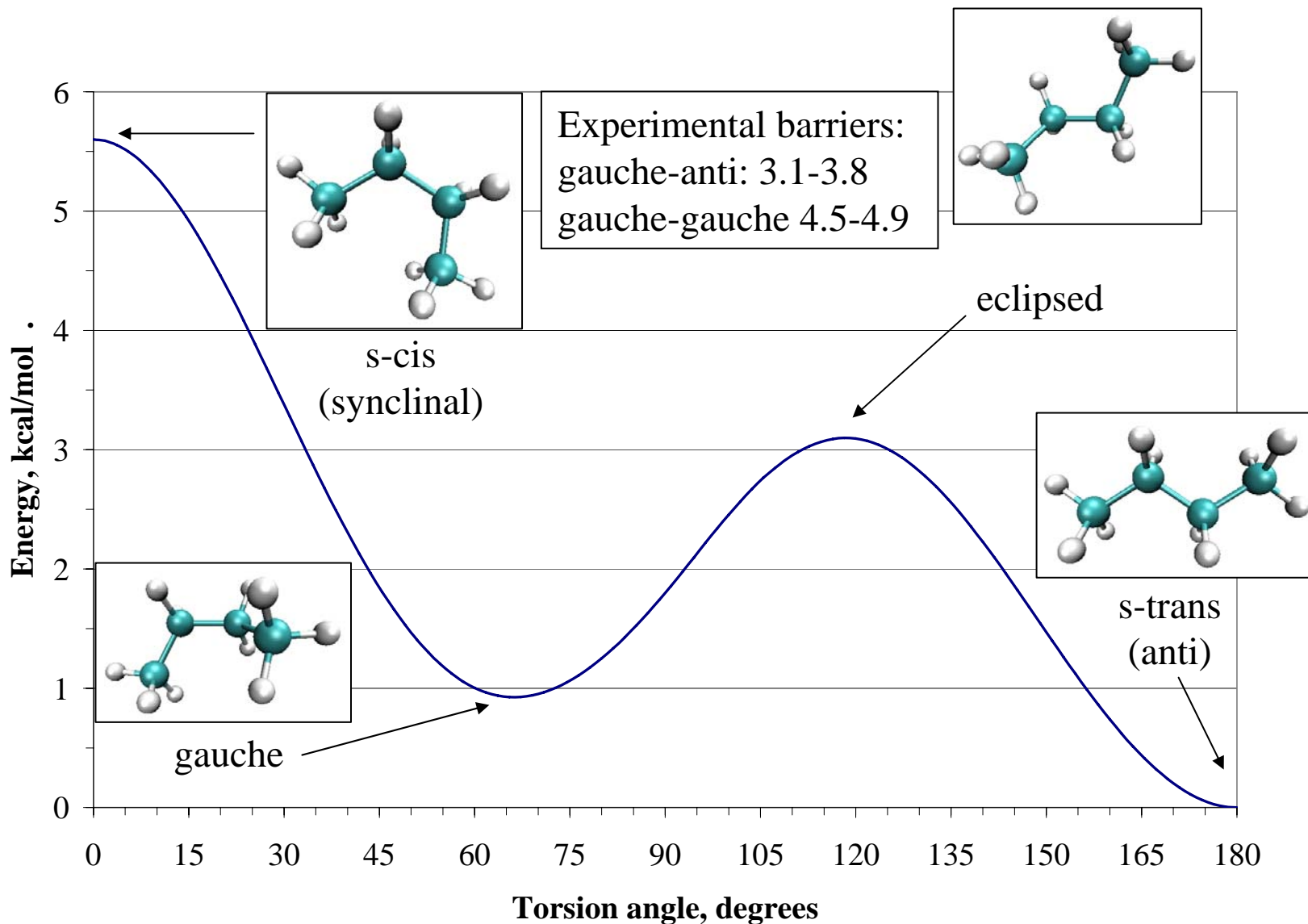
- Isomerization of 1-butene - *syn* \leftrightarrow *skew* (*anti*)



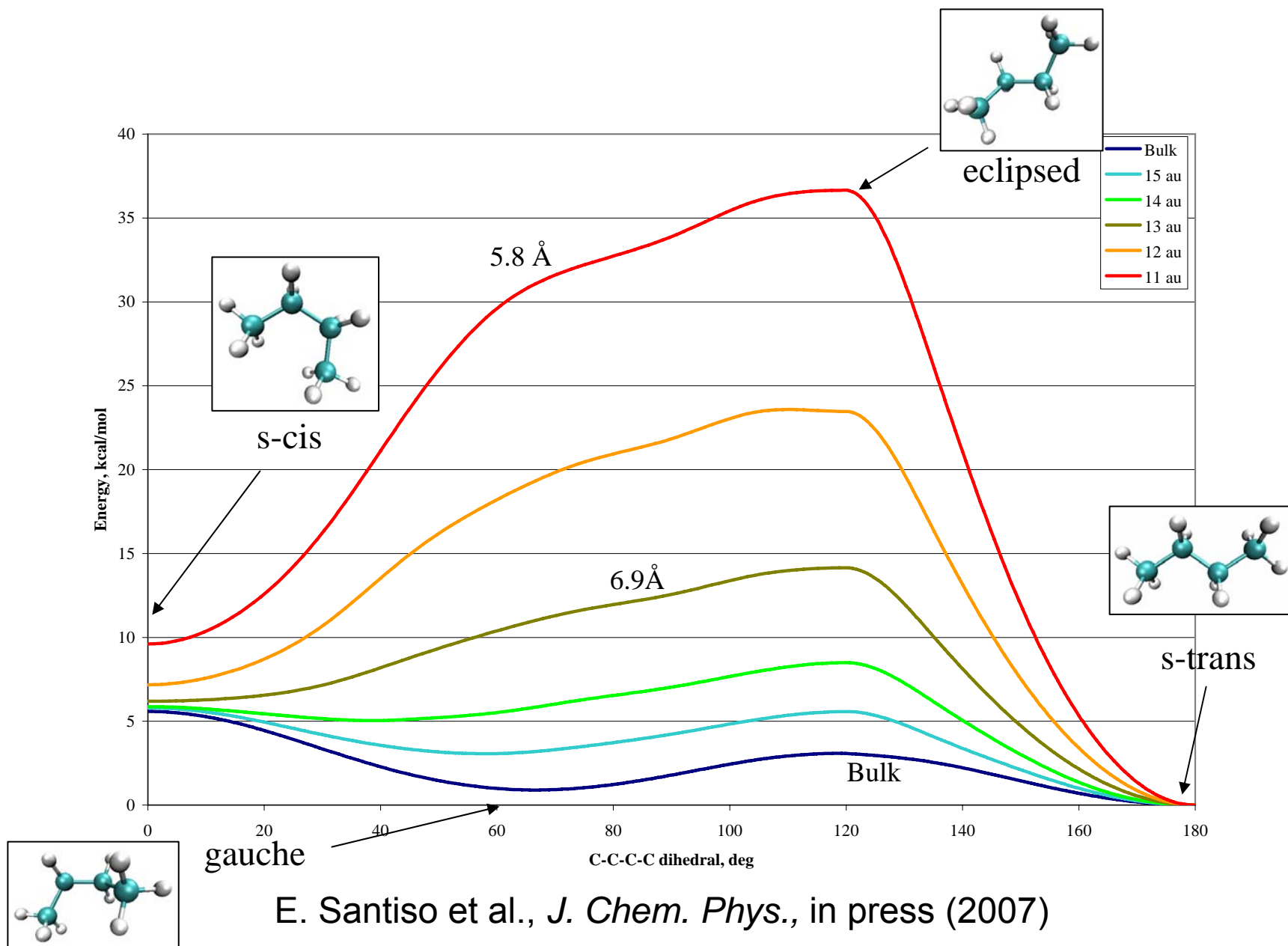
- Isomerization of 1,3-butadiene - *s-trans* \leftrightarrow *gauche* (*s-cis*)



Geometry Effects: Isomerization of n-Butane in the Bulk Gas



Isomerization of Butane: Slit Carbon Pores



Effect of confinement on the rate of the s-trans-gauche/s-trans-s-cis transition of n-butane: double exponential effect.

Steric hindrance increases the energy barrier approximately as (Buckingham):

$$\Delta E^\ddagger \approx \Delta E_\infty^\ddagger + P \exp(-r/\rho)$$

ΔE^\ddagger = Activation barrier

ΔE_∞^\ddagger = Activation barrier in bulk

r = Pore width

P, ρ = Parameters

Rate constant grows approximately as (TST):

$$k \approx A \exp\left[-\frac{\Delta E_\infty^\ddagger + P \exp(-r/\rho)}{kT}\right] = A' \exp\left[-P' \exp(-r/\rho)\right]$$

Double exponential!

Can rewrite this as:

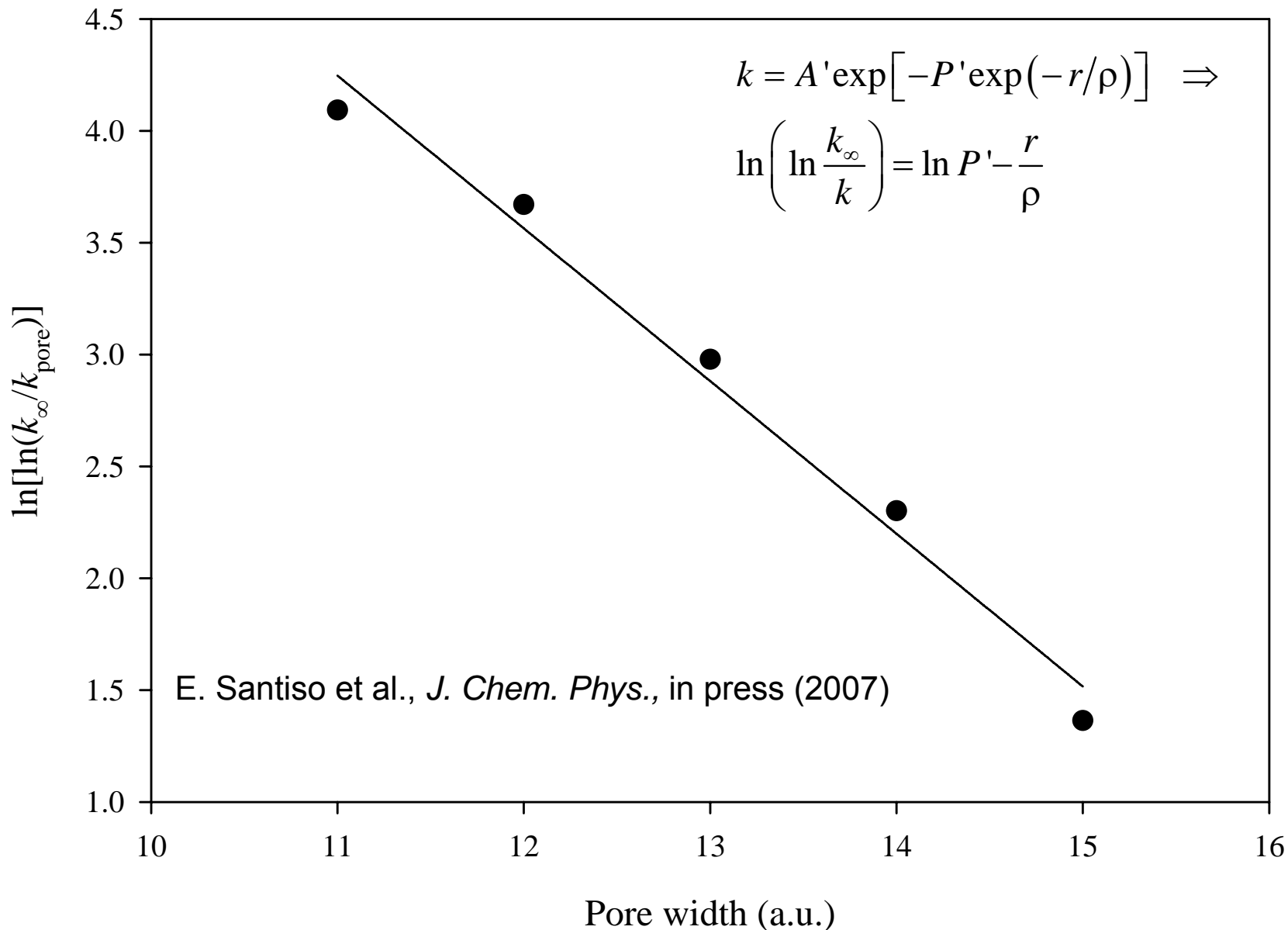
A = Frequency factor

$$\ln\left(\ln \frac{k_\infty}{k}\right) = \ln P' - \frac{r}{\rho}$$

k_∞ = Rate constant in the bulk

Therefore, a plot of $\ln\left(\ln \frac{k_\infty}{k}\right)$ vs. pore size should be approximately linear

Effect of confinement on the rate of the s-trans-gauche/s-cis transition of n-butane: double exponential effect.



Geometric constraints

- For pore sizes comparable to the molecular size ($\sim 3:1$), confinement effects on the torsional potential become important
- Despite having completely different bulk torsional potentials, both n-butane, 1-butene and butadiene become “cis and trans” in the smaller pores. The geometric constraint of the walls favors reactions for which the transition state is near planar (cis, trans), and hinders reactions for which it is non-planar (eclipsed) – shape catalytic effect.
- The geometric constraint of the walls leads to a remarkable “double exponential” variation of reaction rate with pore width.

HYDROGEN GENERATION AND STORAGE

- Economical ways to generate and store hydrogen are crucial steps towards the hydrogen economy and fuel-cell technologies.
- Commercial production of hydrogen by steam reforming or partial oxidation suffers from several drawbacks, in particular the formation of CO and CO₂.
- No existing approach for hydrogen storage satisfies all of the efficiency, size, weight, cost and safety requirements.
- We are studying alternative routes to H₂ production and storage, using carbon-materials as substrates, decorated with transition metal atoms:
 - promising for high-capacity H₂ storage¹
 - avoid production of CO or CO₂ (from H₂O or CH₄ decomposition)
 - generation and efficient storage of H₂
 - reversible hydrogen uptake/release at practical temperatures
 - objective is to design an optimal surface for H₂ production/storage

¹ e.g. T. Yildirim and S. Ciraci, *PRL* **94**, 175501 (2005). [carbon nanotube with Ti]

HYDROGEN GENERATION

- (1) Water gas shift rx (main source):
$$\text{CH}_4 + 2\text{H}_2\text{O} = 4\text{H}_2 + \text{CO}_2$$
- (2) Methane dissociation: $\text{CH}_4 = \text{C} + 2\text{H}_2$
- (3) Water dissociation: $\text{H}_2\text{O} = \text{H}_2 + \text{O}$

Rx (1) is current production method. However, CO_2 is produced, and it relies on fossil fuels

Rx (2) produces no CO_x and is feasible at reasonable temperatures. However, based on a fossil fuel

Rx (3): Advantages: (a) no fossil fuel, (b) no CO_2

Disadvantages: (a) thermal splitting requires $T > 2500^\circ\text{C}$ (water must first be excited to the triplet spin state, ~ 45 kcal/mol); activation energy is ~ 125 kcal/mol; (b) H_2 yield is only about 15-20%; (c) produces O

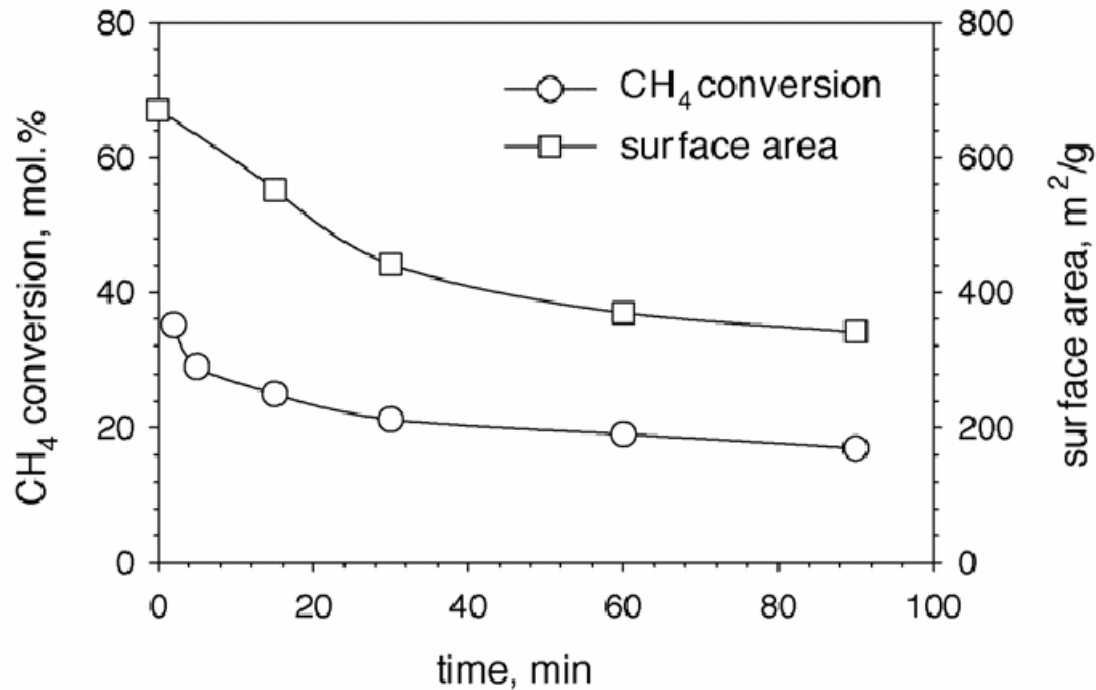
Methane decomposition over carbons, $\text{CH}_4 = \text{C} + 2\text{H}_2$ - experiment

Initial rates of methane decomposition over various carbon materials at 850 °C

Number	Carbon	Surface area (m ² /g)	k ⁰ (mmol/min g)
1	AC, coconut CL	1650	1.67
2	AC, hardwood	1500	2.04
3	AC, phenol resin	1980	1.66
4	CB, black pearls 2000	1500	1.15
5	Graphite, natural	4–6	0.02
6	Graphite, polycrystalline	3–10	0.10
7	Carbon nanotubes	–	0.20
8	Fullerene soot	–	1.90
9	Fullerenes C60/70	–	0.55

k⁰ denotes the initial rate of methane decomposition per unit mass

Methane decomposition over activated carbon, 850 °C



Correlation between methane conversion yield over AC and carbon surface area

Suspended monolayer graphene sheet



Bright-field TEM image of a suspended graphene membrane. The central part (homogeneous and featureless region indicated by arrows) is monolayer graphene.

* Figure reproduced from J. C. Meyer, A. K. Geim, M. I. Katsnelson, K. S. Novoselov, T. J. Booth & S. Roth, “*The structure of suspended graphene sheets*”, Nature **446**, 60 (2007).

Graphene Single Vacancies (GSV): *In situ* observation of vacancy formation in a graphene layer by high-resolution TEM *

a, b, HR-TEM images of a single-walled carbon nanostructure recorded before electron irradiation (**a**) and after 320 s of irradiation (**b**). Intensity profiles (insets) between the two arrows illustrate the contrast measured at the carbon vacancies.

c, d, Atomistic models (**c**) and simulated HR-TEM image (**d**) for a graphene layer with an adatom, unrelaxed vacancies (V1 and V2) and a 5–8–5 rearrangement. Squares indicate the location of the vacancy.

e, Atomic model and simulated HR-TEM image with three mono-vacancies, giving the best match to the experimentally observed defect structures (**b**, inset). Scale bar, 2 nm.

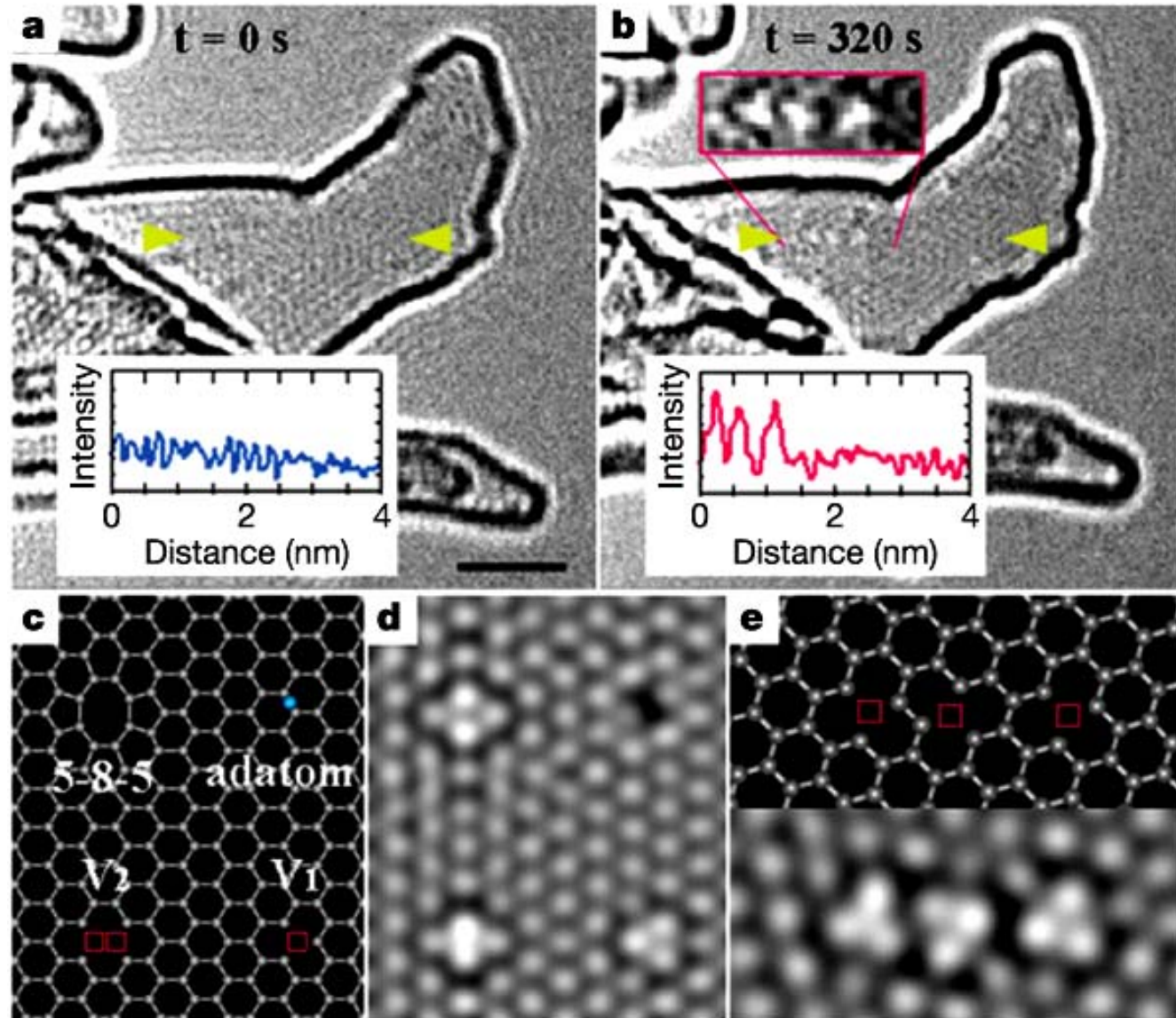
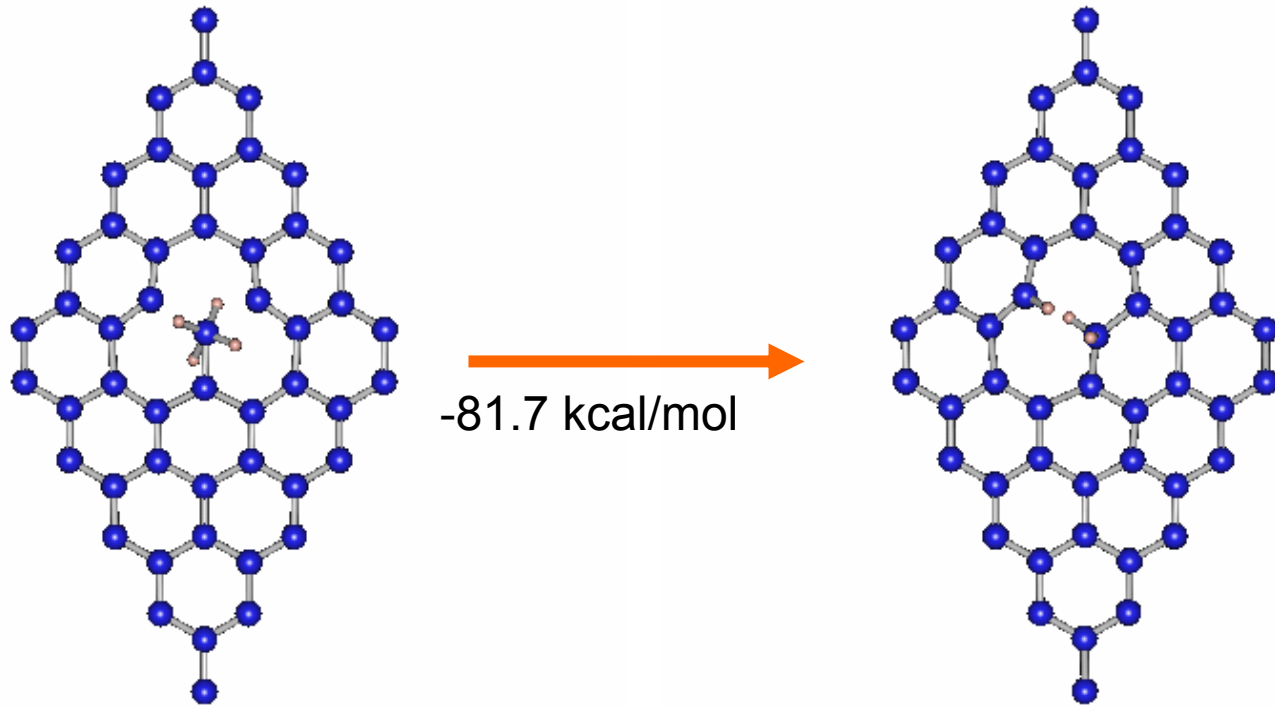


* Figure reproduced from A. Hashimoto, K. Suenaga, A. Gloter, K. Urita, and S. Iijima, “Direct evidence for atomic defects in graphene layers”, *Nature* **430**, 870 (2004).

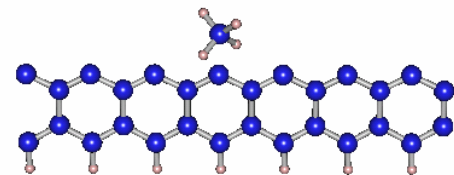
Graphite-single vacancy-CH₄



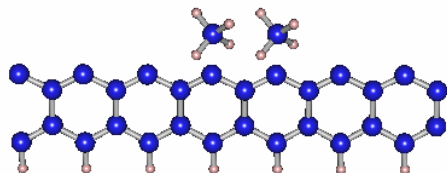
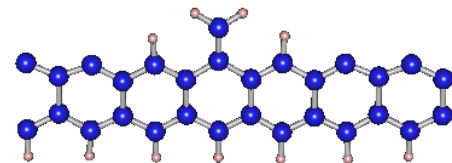
Methane decomposition. But catalytic sites disappear, no H₂. Similar results for nanotubes.

CH₄ decomposition over zigzag edge

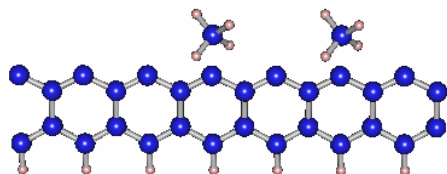
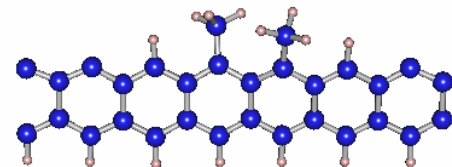
Increasing of methane pressure



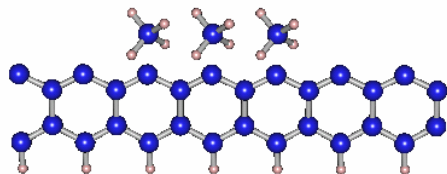
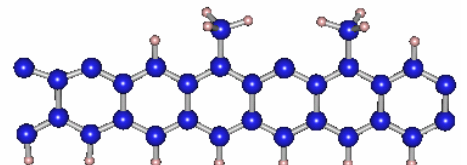
-170.6 kcal/mol



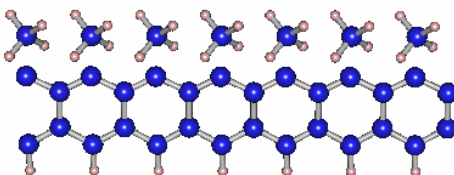
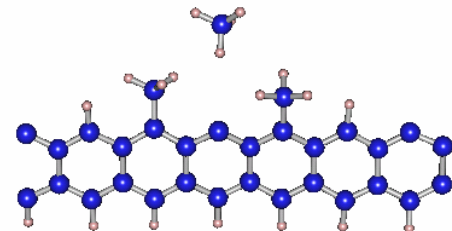
-238.9 kcal/mol



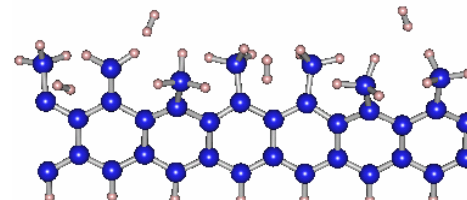
-250.3 kcal/mol



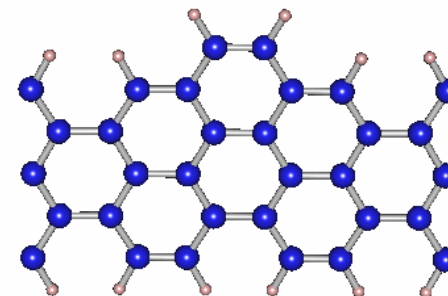
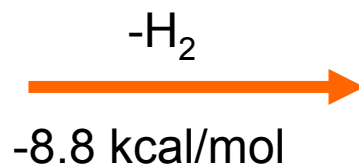
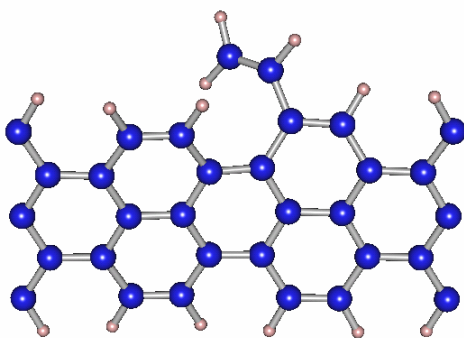
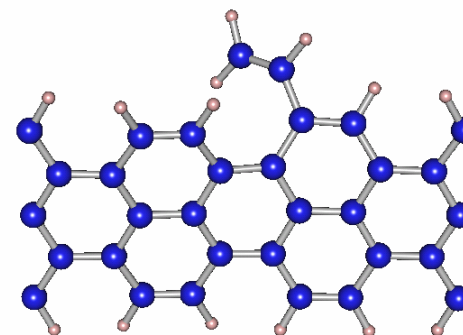
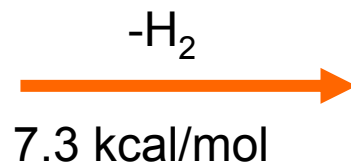
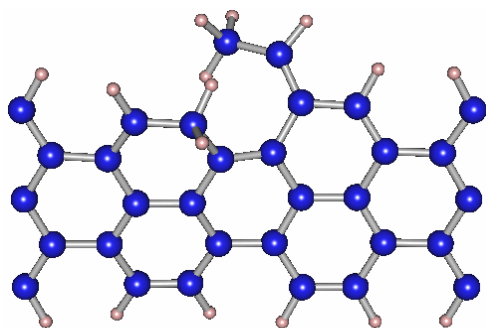
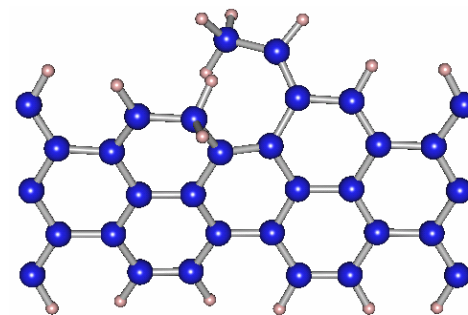
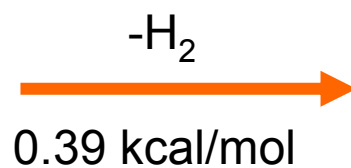
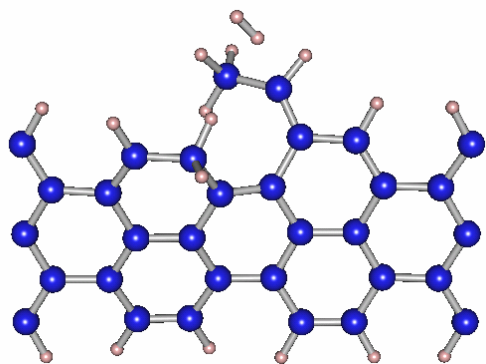
-250.7 kcal/mol



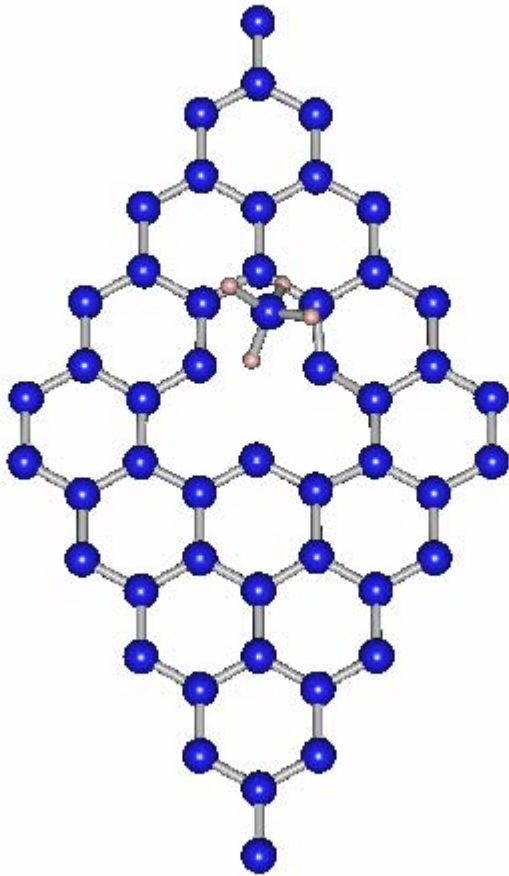
-282.9 kcal/mol



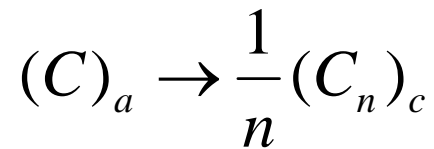
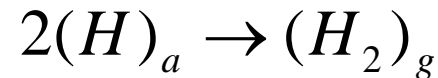
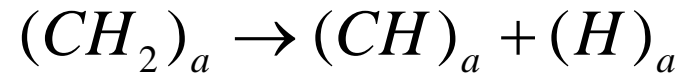
Growth of armchair edge



CH₄ decomposition over vacancy in graphene



Stepwise dissociation reactions:



a: adsorbed species

g: gaseous species

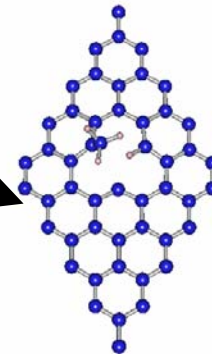
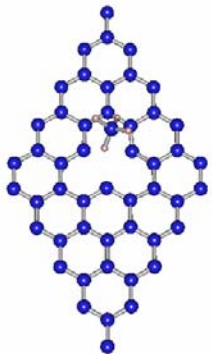
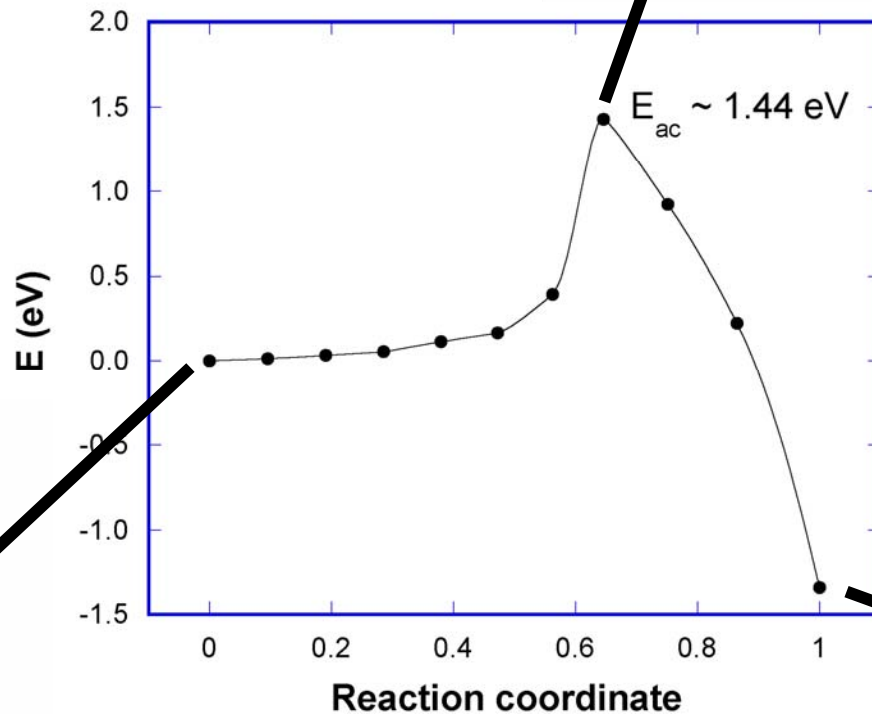
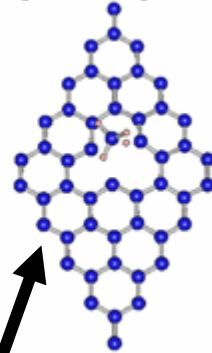
c: crystalline phase

CH₄ decomposition over vacancy in graphene

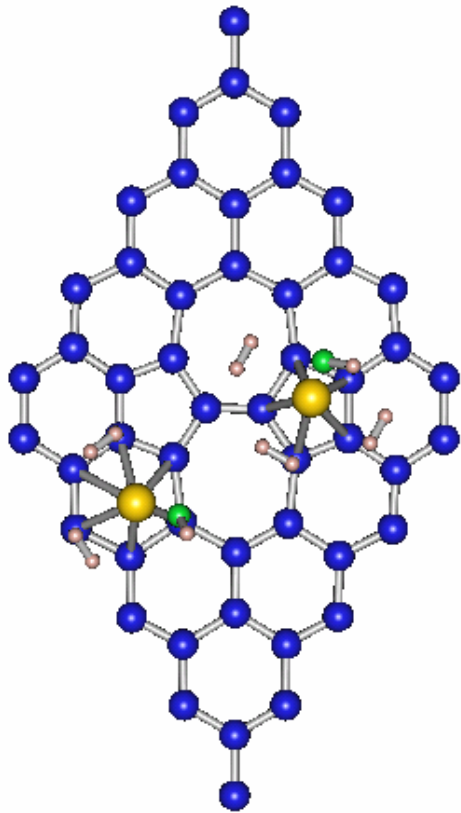
C-H bonding energy in CH₄: 4.56 eV

E_{ac} for non-catalytic thermal decomposition: 3.83-4.488 eV

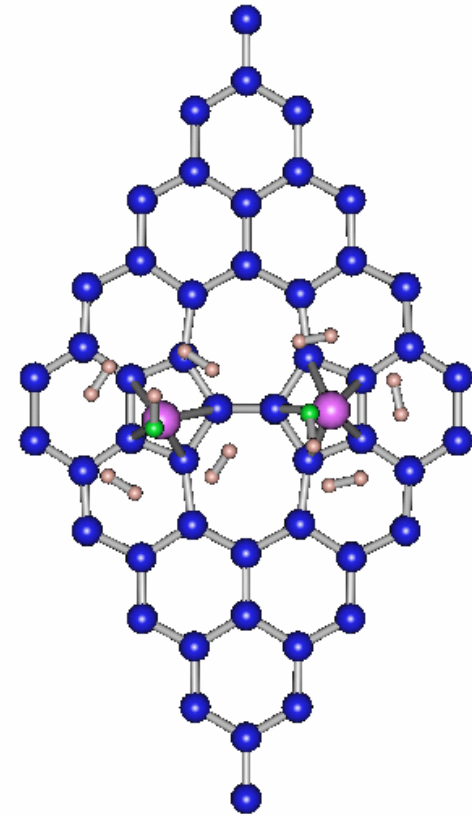
E_{ac} using metal-catalyst: <0.62 eV



H₂ storage over transition metal-decorated graphite with (5-7-7-5) defects



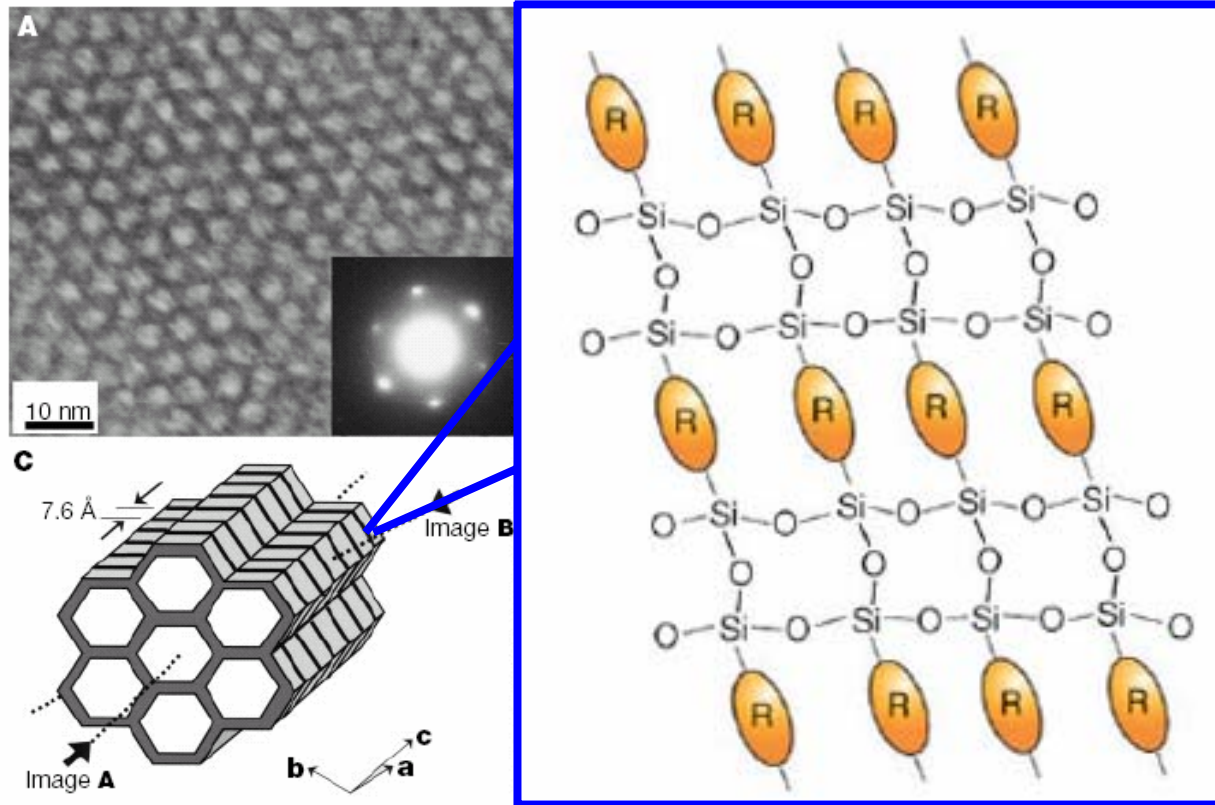
2.5 H₂ per Ti atom



3.5 H₂ per V atom



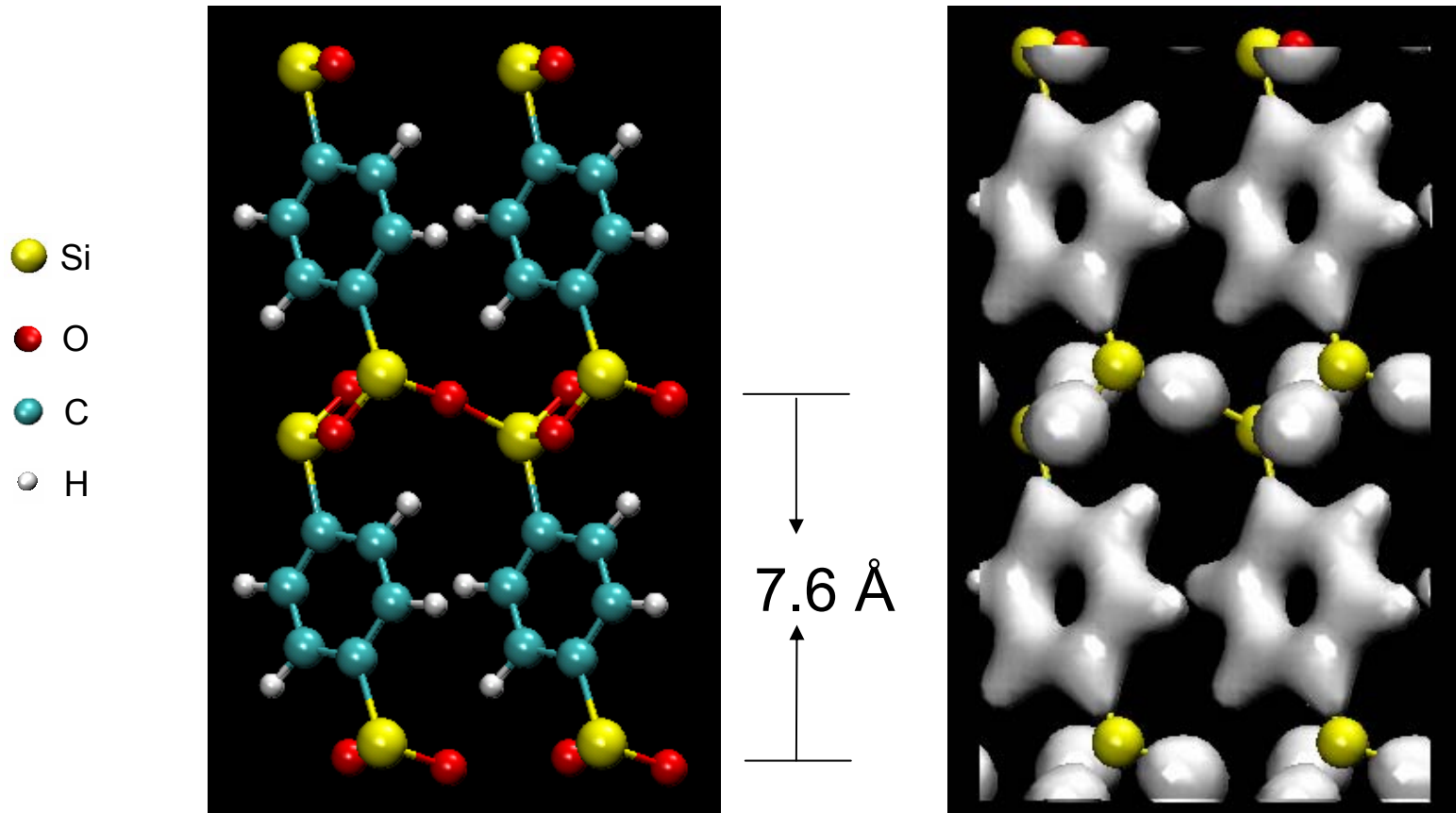
Periodic mesoporous organosilicas (PMO's): CO removal, H₂ storage (?)



HRTEM images of a PMO displaying both meso- and molecular-scale periodicity. (A) hexagonal pore arrangement, (B) pore channels with alternate organic and inorganic regions, (C) schematic structure model.

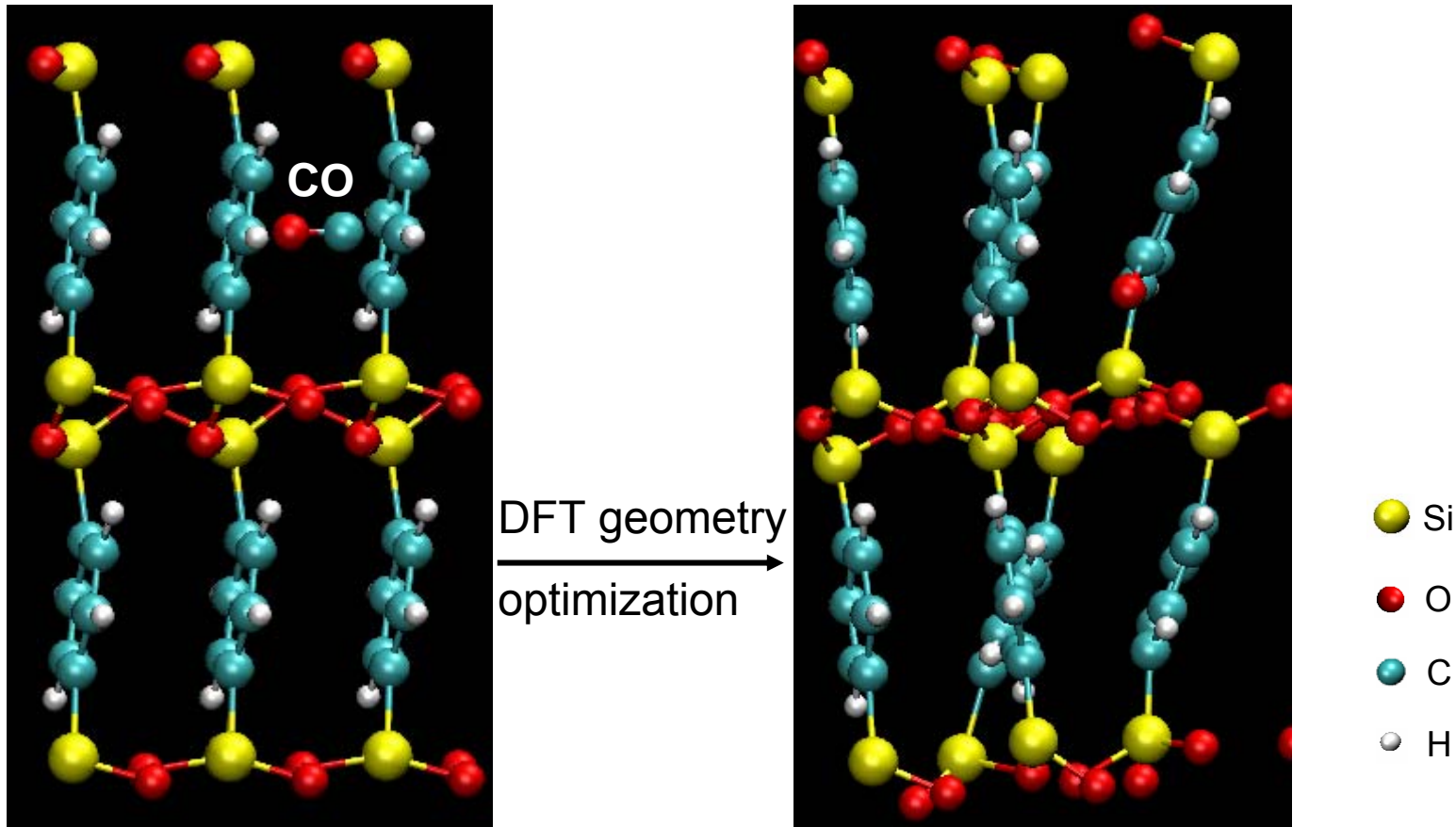
Inagaki *et al.*, *Nature* 416, pp304-307 (2002)

Pore wall of benzene-silica hybrid PMO



Alternate hydrophilic silicate layers and hydrophobic benzene layers in the pore wall, potential applications include improved selectivity, activity of catalysis, separation, sensing and enhanced opto-electrical efficiency of confined molecules and clusters.

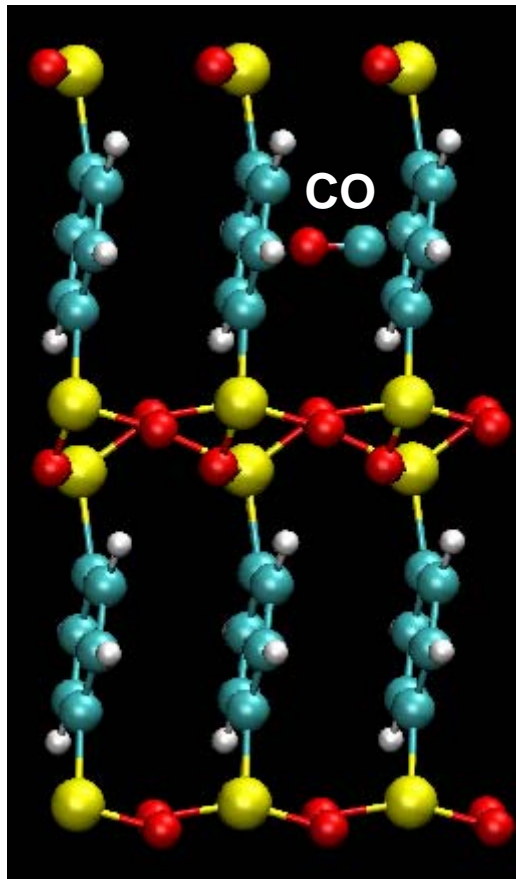
Chemisorption of CO in benzene-silica hybrid PMO



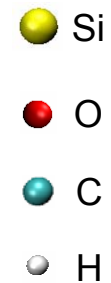
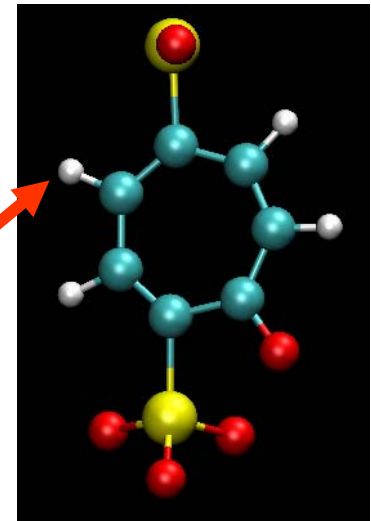
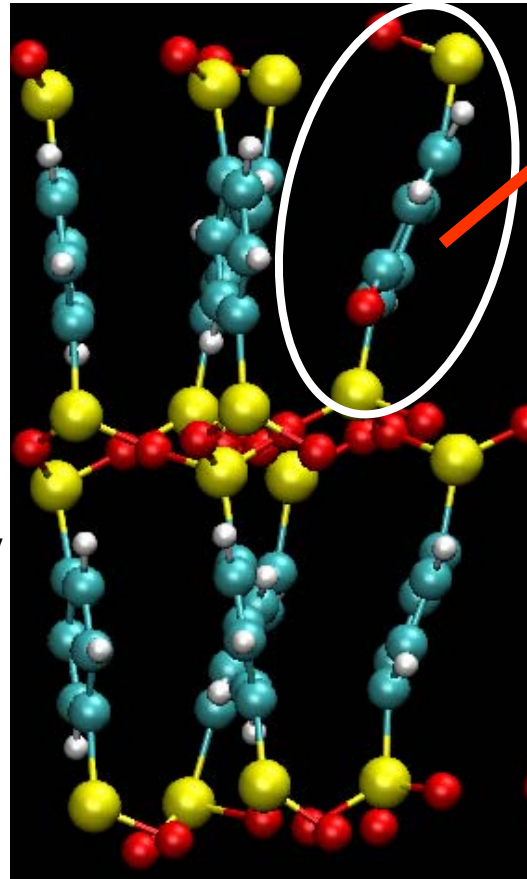
➤ DFT - GGA: BLYP functionals, plane wave plus Vanderbilt ultrasoft-pseudopotentials.

➤ CPMD, © IBM Corp. 1990-2003, © MPI für Festkörperforschung Stuttgart 1997-2001, <http://www.cpmd.org>

Chemisorption of CO in benzene-silica hybrid PMO



DFT geometry
optimization



CO molecule breaks C-C bond in benzene ring and forms new C-C bond.

Conclusions

- The catalytic activity of carbon for methane or water decomposition is governed by the existence of high-energy sites (dangling bonds). However, transition metal atoms are needed to achieve reasonable reaction temperatures.
- The catalytic sites in defective carbon can be largely regenerated by the deposition of carbon decomposed from methane, to make the hydrogen production a continuous process.
- Currently we are carrying out phonon calculations which will permit us to calculate the free energies and reaction paths for these reactions for a range of higher temperatures.
- PMO's offer potential applications for removal of toxic gases, such as CO, and, when decorated with transition metal atoms, may be useful for hydrogen storage.

Future Needs

- Much closer integration of theory and experiment.
- More realistic atomic models of nanoporous catalysts and supports; inclusion of defects, pore tortuosity and connectivity, wall heterogeneity and roughness